Journal of Colloid and Interface Science 440 (2015) 245–252

Contents lists available at ScienceDirect

Journal of Colloid and Interface Science

www.elsevier.com/locate/jcis

Association of anionic surfactant and physisorbed branched brush layers probed by neutron and optical reflectometry

Xiaoyan Liu [a,*], Andra Dedinaite [a,b], Tommy Nylander [c], Aleksandra P. Dabkowska [c,d], Maximilian Skoda [e], Ricardas Makuska [f], Per M. Claesson [a,b]

[a] KTH Royal Institute of Technology, School of Chemical Science and Engineering, Department of Chemistry, Division of Surface and Corrosion Science, Drottning Kristinas väg 51, SE-100 44 Stockholm, Sweden
[b] SP Technical Research Institute of Sweden, Chemistry, Materials and Surfaces, P.O. Box 5607, SE-114 86 Stockholm, Sweden
[c] Physical Chemistry, Lund University, P.O. Box 124, SE-221 00 Lund, Sweden
[d] The Nanometer Structure Consortium, Lund University, P.O. Box 118, SE-221 00 Lund, Sweden
[e] ISIS, STFC, Rutherford-Appleton Lab, R3 2.3 Chilton, Didcot OX11 0QX, United Kingdom
[f] Department of Polymer Chemistry, Vilnius University, Naugarduko 24, LT-03225 Vilnius, Lithuania

ARTICLE INFO

Article history:
Received 2 September 2014
Accepted 2 November 2014
Available online 11 November 2014

Keywords:
Polymer brush layer
Diblock copolymer
SDS
Adsorption
Polyelectrolyte-surfactant complex
Optical reflectometry
Neutron reflectivity

ABSTRACT

Pre-adsorbed branched brush layers were formed on silica surfaces by adsorption of a diblock copolymer consisting of a linear cationic block and an uncharged bottle-brush block. The charge of the silica surface was found to affect the adsorption, with lower amounts of the cationic polyelectrolyte depositing on less charged silica. Cleaning under basic conditions rendered surfaces more negatively charged (more negative zeta-potential) than acid cleaning and was therefore used to increase polyelectrolyte adsorption. The structure of adsorbed layers of the diblock copolymer was as determined by neutron reflectometry found to be about 70 nm thick and very water rich (97%). Interactions between the anionic surfactant sodium dodecylsulfate (SDS) and such pre-adsorbed diblock polymer layers were studied by neutron reflectometry and by optical reflectometry. Optical reflectometry was also used for deducing interactions between the individual blocks of the diblock copolymer and SDS at the silica/aqueous interface. We find that SDS is readily incorporated in the diblock copolymer layer at low SDS concentrations, and preferentially co-localized with the cationic block of the polymer next to the silica surface. At higher SDS concentrations some desorption of polyelectrolyte/surfactant complexes takes place.

1. Introduction

Interactions between polyelectrolytes and oppositely charged surfactants have been an active research field for many years [1–5]. It is an interesting and challenging topic, not only from a fundamental point of view, but also because of numerous applications in a variety of products like cosmetics and personal care, household care, coatings, and formulations for active ingredients such as drugs and pesticides. In these applications both bulk and surface association of oppositely charged polyelectrolytes and amphiphilic molecules have to be considered, and these aspects have been investigated both experimentally and theoretically [6–8]. Synergistic effects between the components are utilized to control deposition and to achieve high efficiency [9]. The outcome of the association is highly dependent on the polyelectrolyte structure, and thus even though much has been learned about association between linear polyelectrolytes and surfactants, less is known for other polyelectrolyte architectures. In this work we focus on association between anionic surfactants and a diblock copolymer consisting of a linear cationic block and an uncharged bottle-brush block with poly(ethylene oxide) side chains [10].

Polyelectrolytes with poly(ethylene oxide) (PEO) side chains have attracted attention [11,12] due to PEO's efficacy in stabilizing colloidal particles, which is essential in many applications [13]. Surface and bulk association of polyelectrolytes with PEO side chains and oppositely charged surfactants have been investigated by a wide variety of experimental techniques including electron microscopy, fluorescence emission spectroscopy [14], ellipsometry, neutron reflectometry [7], surface force apparatus [6], scattering and NMR [15], and QCM-D (quartz crystal microbalance with dissipation) [16]. However, there is still much to be learned about the mechanism of adsorption and formation of complexes between surfactants and oppositely charged polyelectrolytes with PEO side chains at interfaces [7]. This is particularly the case when

* Corresponding author. Fax: +46 8 208998.
E-mail addresses: xiaoyanl@kth.se (X. Liu), maximilian.skoda@stfc.ac.uk (M. Skoda).

http://dx.doi.org/10.1016/j.jcis.2014.11.002
0021-9797/

considering the intriguing branched brush-like polymer architecture that is the focus of the present study.

A polymer brush layer can be described as a dense array of polymer chains end-tethered to a flat surface. Alexander and deGennes showed, using scaling arguments, that the chains in dense brush layers tend to be strongly stretched as a result of excluded volume interactions [17]. A similar picture is obtained from lattice mean-field calculations [18] and simulations [19]. These excluded volume interactions not only cause the chains to stretch, but also oppose penetration of particles and polymers into the brush [17,20]. Both the length of the polymer chain and the grafting density have a large influence on layer properties. For instance, it has been shown that the adsorption of cationic surfactants into an anionic polymer brush layer with high graft density only results in about 40% of the polyelectrolyte brush counterions being exchanged for surfactant ions, whereas much higher exchange is observed at low grafting densities [21].

A study using an analytical self-consistent-field (SCF) theory has addressed adsorption of anionic surfactant micelles into a nonionic polymer brush layer. The surfactant micelles were treated as nanoparticles, and this model predicts a maximum in adsorbed amount of surfactant as a function of polymer grafting density. This result arises from two competing effects. The amount of polymer to which the surfactants can bind increases with increasing grafting density, but on the other hand the excluded volume interaction at higher grafting densities becomes larger and counteracts adsorption of surfactant micelles [22].

In this work, we use neutron reflectometry to characterize the structure of adsorbed layers of a diblock copolymer consisting of a linear cationic block and an uncharged bottle-brush block, which previously has been shown to be highly efficient in mediating low friction forces in aqueous media [12]. We further consider interactions between pre-adsorbed branched brush layers formed by this polymer and the anionic surfactant sodium dodecylsulfate, SDS, and report data from zeta-potential, optical reflectometry and neutron reflectivity measurements. We show that the charge of the silica surface is affected by the cleaning procedure, which in turn influences the adsorption of the block copolymer.

2. Materials and methods

2.1. Materials

The diblock copolymers [$(METAC)_m$-*b*-$(PEO_{45}MEMA)_n$] was synthesized by AGET ATRP (activators generated by electron transfer, atom transfer radical polymerization) as described elsewhere [10]. In this representation METAC stands for methacryloxyethyl trimethylammonium chloride, and $PEO_{45}MEMA$ stands for poly(ethylene oxide)methylether methacrylate. The number average degree of polymerization of the METAC block is 90, whereas that of the non-ionic block is 100, with a high polydispersity. The number average polymer molecular weight is 230 kDa. The structure of the diblock copolymer is provided in Fig. 1, and we note that the *diblock* character is distinctly different to that of the *random* copolymers formed by similar structural units that have been used in most previous studies [23,24]. We also investigated each block separately using $(METAC)_m$ with number average molecular weight of 18.7 kDa, average number of segment ($m = 90$) and polydispersity index of 1.25, and $(PEO_{45}MEMA)_n$ with number average molecular weight of 230 kDa and average number of segment ($n = 113$).

Sodium chloride (NaCl, BioXtra, ⩾99.5%), sulfuric acid (H_2SO_4, ACS reagent, 95.0–98.0%), sodium dodecylsulfate (SDS, BioXtra, >99%), hydrogen peroxide (H_2O_2, ACS reagent, 30 wt.% in H_2O), hydrochloric acid (HCl, 37 wt.% in H_2O, 99.999% trace metals basis),

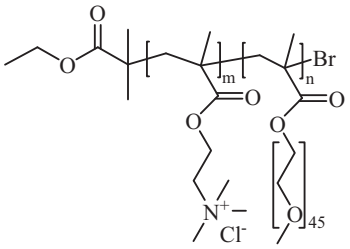

Fig. 1. Molecular structure of $(METAC)_m$-*b*-$(PEO_{45}MEMA)_n$.

and sodium hydroxide (NaOH, BioXtra, ⩾98%) were purchased from Sigma–Aldrich. Potassium chloride (KCl, Molecular Biology Grade) was purchased from VWR International Ltd. The water was purified by employing a Milli-ROPls unit connected to a Milli-Q plus 185 system and filtered through a 0.2 μm Millipak filter at 25 °C. The resistivity of the water was 18.2 MΩ cm and the organic content was less than 3 ppb. Thermally oxidized silicon wafers with a 100 nm thick SiO_2 layer (Wafer Net, Germany) were used in optical reflectometry measurements.

2.2. Methods

2.2.1. Hellmanex cleaning

The silicon wafers were cut to size and cleaned by immersion in alkaline 2% Hellmanex (Hellma GmbH) solution (pH ∼ 12) for 30 min followed by rinsing several times with Milli-Q water. The wafers were left overnight in Milli-Q water before measurement.

2.2.2. Piranha cleaning

A diluted Piranha solution consisting of a 5:4:1 mixture of H_2O, H_2SO_4 and H_2O_2 was used. This solution removes most organic matter due to the strong oxidizing power, and it hydroxylates the silica surface [25]. The wafers cut to size or the silicon blocks used for neutron reflectometry were immersed in the Piranha solution for 15 min at a temperature of 82 ± 2 °C followed by rinsing several times with excessive amounts of Milli-Q water. The wafers were left overnight in Milli-Q water before measurements.

2.2.3. SurPASS

The streaming potential/current method was used to determine the ζ-potential of the silica wafers [26]. In this study, we used the SurPASS instrument (Anton Paar GmbH, Graz, Austria), which has been described in detail elsewhere [27]. Measurements were performed in 1 mM KCl solution using two silica substrates (10 × 20 mm) arranged parallel to each other and separated by a 100 ± 5 μm gap in the measuring cell. The range of titrations was carried out from pH 1.8 to 9. The measurements were operated separately, above and below pH 5.6, respectively. The ζ-potential was calculated according to the Helmholtz–Smoluchowski relation [28]:

$$\zeta = \frac{I\lambda\eta L}{\Delta P \varepsilon_r \varepsilon_0 H} \quad (1)$$

where I is the streaming current, ΔP the measured pressure difference, λ the specific conductivity of the electrolyte solution in the channel, η the viscosity, ε_r and ε_0 are the dielectric constant and the vacuum permittivity, L and H are channel length and width, respectively.

2.2.4. Optical reflectometry

The adsorption of the polymers on thermally oxidized silicon wafers was investigated by optical reflectometry [29]. Stagnation point adsorption reflectometry experiments were performed in a temperature-controlled room at 25 ± 1 °C. Linearly polarized light

is reflected at the Si/SiO_2-water interface at an angle close to the Brewster angle. The reflected light is split into its parallel and perpendicular polarization components I_p and I_s, and the respective intensities are recorded by photodiodes. The ratio I_p/I_s, defined as the signal (S), is continuously recorded during an experiment. The change in the signal (ΔS) upon adsorption is related to the adsorbed mass, Γ, via [29]:

$$\Gamma = \frac{1}{A_s} \times \frac{\Delta S}{S_0} \quad (2)$$

The parameter A_s, also known as the sensitivity factor (relative change in S per unit surface excess), is determined by treating the system as a four-layer optical model where each layer is characterized by its thickness (t), and refractive index (n): Si (n_{Si}, t_{Si})-SiO_2 (n_{SiO2}, t_{SiO2})-adsorbing layer (n_{layer}, t_{layer})-aqueous medium (n_{water}) within the framework of Fresnel reflectivity theory [30]. The sensitivity factor also depends on the refractive index increment (dn/dc) of the adsorbing species and this was considered using the procedure suggested by Dedinaite and Bastardo [31].

2.2.5. Neutron reflectometry

Neutron reflectivity measurements were conducted on the INTER reflectometer (ISIS Spallation Neutron Source, Rutherford Appleton Laboratory, Didcot, UK) using the time-of-flight mode. Data were collected by illuminating the sample with a polychromatic neutron beam (wavelength range of 1.5–15 Å) at two incident angles (0.7° and 2.3°) to give a range of Q from 0.009 to 0.33 $Å^{-1}$. The data were corrected by beam transmission in air and scaled to a reflectivity value of 1 at total reflection. The neutron reflectivity of each sample was measured as a function of the neutron momentum transfer, Q ($Q = 4\pi \sin\theta/\lambda$, where θ is the grazing angle of incidence and λ is the wavelength).

The sample cell consisted of a large polished silicon crystal ($8 \times 5 \times 1.5$ cm) clamped against a flow reservoir/trough machined out of polyether ether ketone (PEEK) with a volume of about 2 mL. The silicon crystal was clean by the Piranha treatment and then treated with NaOH solution at pH 10 for 30 min. This less alkaline solution, compared to 2% Hellmanex solution, was used to avoid roughening of the surface due to the alkaline treatment. The incident beam entered through the silicon block, and was reflected at the interface between the silicon substrate and the aqueous bulk phase.

A theoretical neutron reflectivity profile was fitted to the experimentally determined profile. This theoretical profile was calculated using a simulated scattering length density profile based on a surface structure consisting of slabs. Each slab is defined by its scattering length density (SLD, ρ), thickness and roughness, and these quantities were adjusted to obtain an optimal fit using the Motofit program [32] that employs the optical matrix formalism. The χ^2 value obtained from the simultaneous fitting was noted. We applied the simplest possible model, using the least number of parameters that adequately described the data. When an additional layer was required to fit the data, the difference in quality of the fit with and without this layer was assessed by comparing a qualifier based on the χ^2 value and taking into account the number of parameters [33,34].

The SLD of the polymer (ρ_{poly}), substrate and solvent ($\rho_{solvent}$) are provided in Table 1. The SiO_2 on the bare silicon block was modeled as a single slab. After addition of polymer, the interface was modeled assuming two slabs, one being the SiO_2 (as determined from the bare block) and the other being a diffuse layer of polymer. The polymer volume fraction (Φ_{poly}) was calculated from the fitted SLD of the layer (ρ_{layer}):

$$\rho_{layer} = \rho_{solvent}\Phi_{solvent} + \rho_{poly}\Phi_{poly} \quad (3)$$

where the $\Phi_{solvent}$ and Φ_{poly} are the volume fractions of the solvent and polymer, respectively. Similarly, after addition of SDS, we obtain NR data in which the isotopic composition of the surfactant and/or the solvent changes. Thus, from the fitted SLD of each layer for the three contrasts, we can determine the volume fractions of each component.

From Φ_p the surface excess, Γ, can be obtained as:

$$\Gamma = \frac{d\Phi_p}{(N_a V_p)/M_{wp}} = \frac{d\Phi_p}{v_p} \quad (4)$$

where d is the thickness of the layer, N_a, is Avagadro's number, M_{wp} is the polymer molecular weight, V_p is the molecular volume and v_p is the partial specific volume of the polymer, i.e. the inverse of the density. The corresponding relation can be derived for the surfactant.

3. Results and discussion

In this section we first discuss how the surface treatment during cleaning affects the silica surface charge density as determined by electrokinetic measurements. We demonstrate that the cleaning process affects the surface charge, which in turn influences adsorption of cationic polyelectrolytes. Next, we discuss the structure of the layer formed by $(METAC)_m$-*b*-$(PEO_{45}MEMA)_n$ on silica as determined by neutron reflectometry. Thereafter, we consider how SDS affects pre-adsorbed layers of $(METAC)_m$-*b*-$(PEO_{45}MEMA)_n$.

3.1. Effects of surface treatment

3.1.1. Zeta potential of silica surfaces

The ζ-potential as a function of pH for silica surfaces cleaned by either alkaline Hellmanex or strongly acidic Piranha solution is shown in Fig. 2. As expected, the zeta potential decreases with increasing pH for both surfaces due to increasing dissociation of surface silanol groups. We also note that at the same pH value, the ζ-potential for the surface cleaned by Piranha solution is less negative than that of the surface cleaned by using Hellmanex. This suggests that the number of silanol groups and/or the type of silanol groups present on the surface differ [38]. The isoelectric point is found around pH ~ 2 for the surface cleaned by Hellmanex, whereas a value as high as pH ~ 4 is found for the surface cleaned by Piranha. The adsorption studies reported in the following sections were all done at pH ~ 6. At this pH-value the ζ-potential for silica cleaned by Hellmanex is −100 mV whereas that of silica cleaned by Piranha solution is −60 mV. Thus, cleaning with Hellmanex results in a more negatively charged surface than cleaning with Piranha.

3.1.2. Adsorption properties

Adsorption of the diblock copolymer, $(METAC)_m$-*b*-$(PEO_{45}MEMA)_n$, the uncharged bottle-brush block, $(PEO_{45}MEMA)_n$, and the cationic block, $(METAC)_m$, were investigated on both types of silica surfaces by means of optical reflectometry. The results obtained in 10 mM NaCl are summarized in Table 2. The low concentration used for $(METAC)_m$ (1 ppm) was chosen such that the number of charged groups added to the solution was similar to that for the diblock copolymer at a concentration of 50 ppm. We note that the absolute concentration of this highly charged polymer is not expected to affect the adsorbed amount significantly due to the high affinity adsorption isotherm of such polyelectrolytes on silica [39].

The adsorbed mass of the cationic block was found to be 0.36 and 0.28 mg/m^2 on silica surfaces cleaned by Hellmanex and Piranha solution, respectively. Adsorption of the cationic block is predominantly driven by electrostatic interactions between

Table 1
Scattering length densities and other parameters used for the analysis of neutron data.

Material	Molecular formula	Density (mg/ml)	Molecular weight (g/mol)	Molecular volume (Å^3)	Scattering length (10^{-5} Å)	SLD (10^{-6} Å^{-2})
Water	H_2O	1.0	18.02	30	−1.68	−0.56
	D_2O	1.11	20.03	30	19.1	6.35
SDS	$NaC_{12}H_{25}SO_4$		288.4	415[a]	16.0	0.38
	$NaC_{12}D_{25}SO_4$		313.5	415[a]	276	6.66
PEO_{45}	$(C_2H_4O)_{45}$	1.193	1982	276[b]	186	0.67
MEMA	$C_4H_5O_2$	1.193	85.08	118[b]	19.50	1.65
$(PEO_{45}MEMA)_{100}$	$((C_2H_4O)_{45}C_4H_5O_2)_{100}$	1.193	206,700	288,000	20,600[a]	0.71
$(METAC)_{90}$	$(C_9H_{18}O_2N)_{90}$		15,500	25,200[c]	1210[a]	0.48[a]
$(METAC)_{90}$-*b*-$(PEO_{45}MEMA)_{100}$			222,200	313,000	21,800	0.70

[a] Data from Ref. [35].
[b] PEO volume calculated from apparent specific volume in bulk [36], same specific volume was used for MEMA.
[c] METAC monomer volume (0.28 nm^3) estimated from bulk density of METAC [37].

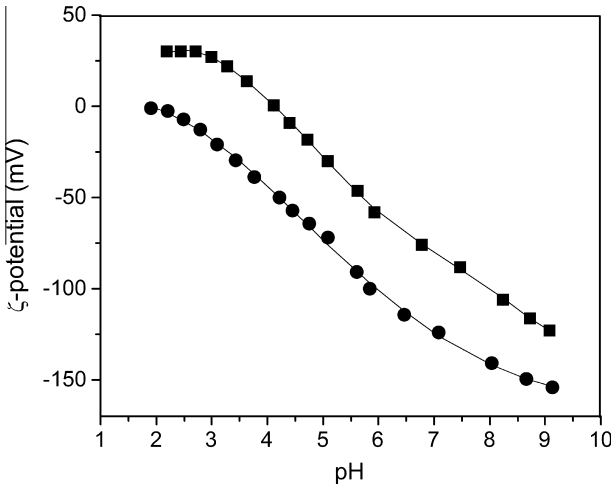

Fig. 2. ζ-potential as a function of pH for silica surfaces cleaned by Piranha (squares) and Hellmanex 2% (circles). The background electrolyte was 1 mM KCl. Error bars based on 2 measurements are small and hidden within the symbols.

Table 2
Adsorbed mass determined by optical reflectometry of $(METAC)_m$, $(PEO_{45}MEMA)_n$, and $(METAC)_m$-*b*-$(PEO_{45}MEMA)_n$ on silica surfaces cleaned by either alkaline solution (2% Hellmanex), Γ_H, or acid (Piranha) solution, Γ_P, respectively. The bulk concentrations of the adsorbing species were 1 ppm for $(METAC)_m$ and 50 ppm for $(PEO_{45}MEMA)_n$ and $(METAC)_m$-*b*-$(PEO_{45}MEMA)_n$. All solutions had a pH ~ 6 and contained 10 mM NaCl.

	Alkaline cleaned Γ_H (mg/m^2)	Acid cleaned Γ_P (mg/m^2)
$(METAC)_m$	0.36 ± 0.03	0.28 ± 0.01
$(PEO_{45}MEMA)_n$	0.95 ± 0.03	0.82 ± 0.1
$(METAC)_m$-*b*-$(PEO_{45}MEMA)_n$	2.4 ± 0.2	1.6 ± 0.1

negatively charged sites on the silica surface and the positive charges carried by $(METAC)_m$. Thus, the higher adsorbed mass found on silica cleaned by Hellmanex is a consequence of the higher negative surface charge density as illustrated by the ζ-potential measurements. This also explains why the adsorbed mass of the diblock copolymer is higher on the Hellmanex cleaned surface, 2.4 mg/m^2 than on the one cleaned by Piranha solution, 1.6 mg/m^2.

The adsorbed mass for the uncharged bottle-brush block was found to be rather similar on silica surfaces cleaned by Hellmanex and Piranha solution. In this case the dominating driving force for adsorption is short-range interactions between PEO and surface silanol groups [24], and apparently this interaction is not significantly altered by the method chosen to clean the surface even though the number of and/or type of silanol groups differ on the two types of silica surfaces.

Table 3
Properties of layers of $(METAC)_m$-*b*-$(PEO_{45}MEMA)_n$ adsorbed on silica from aqueous solutions with no added salt at pH ~ 6 as determined by QCM-D and optical reflectometry. Data from [10].

	$(METAC)_m$-*b*-$(PEO_{45}MEMA)_n$
Adsorbed mass (mg/m^2)	2.75 ± 0.2
Layer thickness (Å)	460 ± 20
Water content (wt%)	94.5 ± 0.2

3.2. Structure of $(METAC)_m$-b-$(PEO_{45}MEMA)_n$ layers on silica

Adsorption of $(METAC)_m$-*b*-$(PEO_{45}MEMA)_n$ on Hellmanex cleaned silica has previously been investigated with QCM-D and optical reflectometry [10], and the key findings are recapitulated in Table 3. We note that these data, unlike those reported in Table 2, were obtained in absence of any added salt. Clearly, the adsorbed layer is thick and has a high water content.

The structure of the diblock copolymer layer adsorbed from a 10 mM NaCl solution on silica surfaces cleaned by Piranha followed by treatment with alkaline solution was evaluated using neutron reflectometry measurements. Measurements were performed in H_2O, D_2O and in contrast match silicon (cmSi, i.e. 62 vol% H_2O and 38 vol% D_2O). The reflectivity profiles obtained for the bare silica substrate is shown in Fig. 3. The three data sets were fitted simultaneously using a three-layer model (silicon-silica-solution). The curves corresponding to the best fit are also shown in Fig. 3 and the parameters are summarized in Table 4. The silica layer was found to be about 9 Å thick, with a water content of 23% and a roughness of 4 Å.

Adsorption of $(METAC)_m$-*b*-$(PEO_{45}MEMA)_n$ results in only small changes in the scattering curves obtained in the D_2O and H_2O contrasts, whereas new features appear in the reflectivity profile in the cmSi contrast, as illustrated in Fig. 4. The presence of rather clear fringes indicates a well-defined layer. The three contrast data sets were simultaneously fitted using a four-layer model (silicon-silica-polymer layer-solution) where the parameters defining the silica layer were fixed from the fitted reflectivity of the bare surfaces. We find that the adsorbed layer is thick, about 700 Å, and that the interface between the layer and the solution is diffuse as illustrated by the large layer roughness of around 40 Å. The water content of the layer is very high and amounts to 97%.

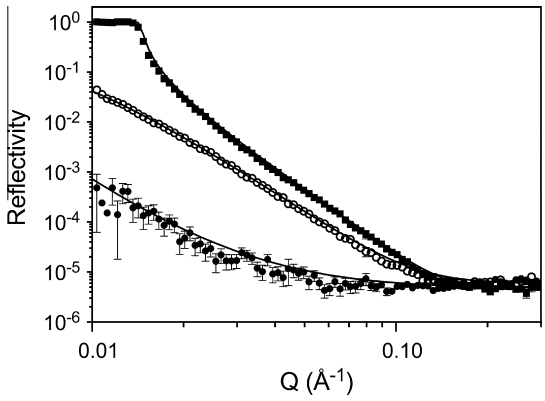

Fig. 3. Neutron reflectivity profiles of the bare silicon/silica substrate measured in D_2O (squares), H_2O (open circles) and cmSi (filled circles), modeled with a single layer of SiO_2. All three contrasts were fitted simultaneously. The best fits are shown as solid black lines. All solutions contained 10 mM NaCl.

Table 4
Structural parameters obtained from fitting of the neutron reflectivity profiles for adsorbed $(METAC)_m$-*b*-$(PEO_{45}MEMA)_n$ layers in 10 mM NaCl.

Parameter	SiO_2	Polymer layer
Thickness (Å)	9 ± 1	700 ± 20
Solvent content ($\Phi_{solvent}$, %)	23 ± 2	97 ± 1
Roughness (Å)	4 ± 1	38 ± 4
Adsorbed amount (mg/m^2)	–	2.6 ± 0.1

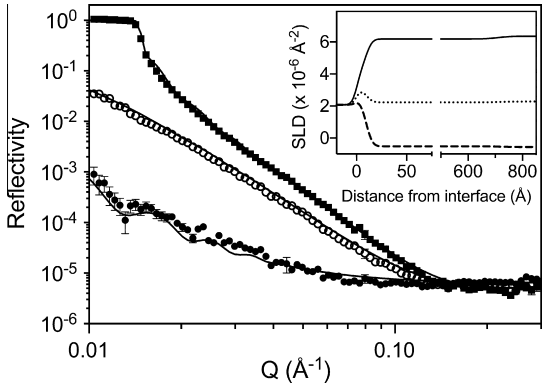

Fig. 4. Neutron reflectivity profiles obtained after adsorption from 50 ppm solutions of $(METAC)_m$-*b*-$(PEO_{45}MEMA)_n$ in D_2O (squares), H_2O (open circles) and cmSi (filled circles). The best fits are shown as solid black lines. All solutions contained 10 mM NaCl. The inset shows the scattering length density profiles, where the solid line is in D_2O, dotted line polymer in cmSi, and the broken line in H_2O.

The structural information obtained by analysis of the neutron reflectivity data is provided in Table 4. We note that the thickness determined by the combination of QCM-D and optical reflectometry and by neutron reflectivity is rather different, whereas the adsorbed amount is almost identical. Here it should be born in mind that the thickness determined by both methods is very dependent on the model employed. We employed the simplest possible model that gives a good fit to the experimental data, which for this case assumes a homogenous layer. A similar homogeneous layer model was also used when evaluating the thickness from QCM-D/optical reflectometry data [10]. We emphasize that the presence of fringes in the NR profile for the cmSi contrast in Fig. 4 makes it likely that the determined thickness value from neutron reflectivity measurements is closer to the true value of the thickness than that reported in Ref. [10]. In addition neutron reflectometry averages the structure over a significantly larger surface area than QCM-D and optical reflectometry (10–20 cm^2 versus $\leqslant$ 1 cm^2) and flow conditions are different in the cell as well. It is also important to emphasize that for a very diluted layer, as in this work, the evaluated thickness of the layer and the volume fraction of polymer in the layer are coupled. Therefore the total adsorbed amount is expected to be more accurately determined than the thickness and the volume fraction profile.

3.3. Interaction between SDS and pre-adsorbed polymer layers

The evaluation of total adsorbed amount in layers consisting of more than one component (in addition to solvent) from optical reflectometry data is complicated due to differences in refractive index increment, i.e. optical response per unit mass, for the different components [40–42]. Due to this complication we present the optical response, as $\Delta S/S$ (Eq. (2)) in Figs. 5 and 7, which is the quantity measured. The refractive index increments for the substances used in this work are provided in Table 5.

3.3.1. $(METAC)_m$-*b*-$(PEO_{45}MEMA)_n$

3.3.1.1. Optical reflectometry. The pre-adsorbed $(METAC)_m$-*b*-$(PEO_{45}MEMA)_n$ layers were exposed to 10 mM NaCl solutions with increasing SDS concentrations. The results are shown in Fig. 5, where the SDS concentration is normalized to the critical micelle concentration (CMC is 6 mM in 10 mM NaCl) [44].

For silica surfaces cleaned in Hellmanex solution, the optical response, i.e. total adsorbed amount, increases in the presence of 0.3 CMC SDS, demonstrating that SDS is incorporated in the layer. No further increase in the optical response can be detected as the SDS concentration is increased to 0.6 CMC, where as a further increase in SDS concentration to 1.2 CMC results in some desorption of polyelectrolyte-surfactant complexes as evidenced by the decrease in the optical response. Next, the layer was rinsed by 10 mM NaCl, which resulted in a further decrease in adsorbed amount as SDS desorbs from the layer.

SDS affects the pre-adsorbed $(METAC)_m$-*b*-$(PEO_{45}MEMA)_n$ layer on acid cleaned silica differently. In this case no maximum in the adsorbed amount with SDS concentration can be noted. Rather, some desorption occurs in the presence of 0.6 CMC SDS, and

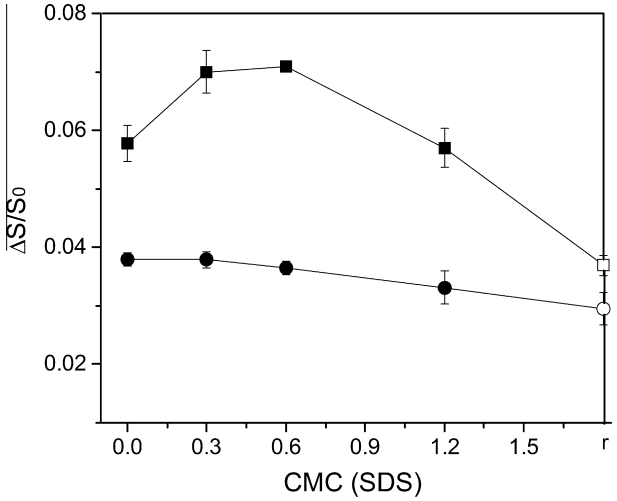

Fig. 5. Optical response $\Delta S/S_0$ (Eq. (2)) as a function of SDS concentration (in 10 mM NaCl) outside a pre-adsorbed $(METAC)_m$-*b*-$(PEO_{45}MEMA)_n$ layer on silica cleaned by alkaline 2 wt% Hellmanex (squares) or, alternatively, by acidic Piranha solution (circles). The diblock copolymer concentration during formation of the pre-adsorbed layer was 50 ppm in 10 mM NaCl, pH ~ 6. The open points denote the values obtained after a final rinsing step with 10 mM NaCl.

Table 5
Refractive index increments.

Substance	dn/dc (mL/g)
$(METAC)_m$-*b*-$(PEO_{45}MEMA)_n$	0.145
$(METAC)_m$	0.158
$(PEO_{45}MEMA)_n$	0.142
SDS	0.126

The dn/dc values for the polymers are taken from Ref. [10], and that for SDS from Ref. [43].

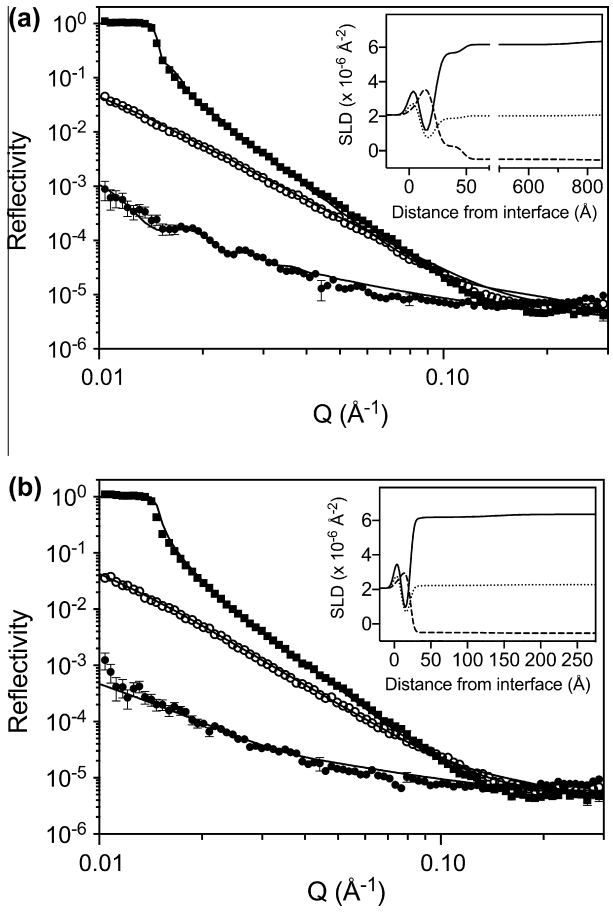

Fig. 6. Neutron reflectivity profiles obtained after addition of (a) 0.3 and (b) 0.6 CMC of SDS to pre-adsorbed $(METAC)_m$-*b*-$(PEO_{45}MEMA)_n$ in D_2O (squares), H_2O (open circles) and cmSi (filled circles). Note that d-SDS was used for the H_2O contrast. The best fits are shown as solid black lines. All solutions contained 10 mM NaCl. The insets show the scattering length density profiles, where the solid line is h-SDS in D_2O and dotted line is h-SDS in cmSi, while the broken line is d-SDS in H_2O.

desorption is enhanced in the presence of SDS above CMC (1.2 CMC). Just as for alkaline cleaned silica a final rinse with 10 mM NaCl results in loss of material from the surface due to SDS desorption.

We clearly have two competing effects. Incorporation of SDS in the layer results in increased adsorbed amount and formation of polyelectrolyte/surfactant complexes at the interface (SDS does not adsorb to silica) [40]. However, SDS also brings negative charges into the layer and the formed polyelectrolyte/surfactant complexes have less electrostatic affinity to the surface than the polyelectrolyte itself. On the alkaline cleaned surface the former process dominates at low surfactant concentrations ($\leqslant$0.6 CMC), whereas desorption predominates at higher SDS concentrations. For acid cleaned silica, which is less charged, desorption appears to dominate at all concentrations investigated. Thus, desorption of diblock copolymer/SDS complexes occurs more readily from the less negatively charged surface, which is consistent with predominance of electrostatic interactions.

3.3.1.2. Neutron reflectivity, NR. In order to separate the adsorbed amount of SDS from that of the polymer, NR experiments were conducted. NR measurements after addition of different amounts of SDS reveal how the surfactant alters the polymer layer. NR data can also give us an indication of where the SDS is located within the adsorbed layer. The recorded data are shown in Fig. 6 for the sequential addition of SDS at two concentrations, 0.3 and 0.6 times the CMC of SDS. The effect is most clearly observed for d-SDS in H_2O where the neutron contrast between the solvent and the surfactant is the largest (see Fig. 6).

To obtain a reasonable fit to the experimental data we have to introduce a four layer model, where the parameters describing the silicon oxide are fixed from fitting the reflectivity from the bare surface (Fig. 3) and the two layers close to the surface contain both polymer and SDS, while the outer layer has only polymer. The results of fitting the three-layer model to the experimental data are summarized in Table 6 and the SLD profile for the different isotopic contrasts are shown as inserts in Fig. 6. The surface excesses of the components in each layer were calculated as described in the experimental section and are expressed in mg/m^2 in Table 6.

The layer closest to the surface represents the anchoring of $METAC_{90}$ and is thin and contains little solvent. The second layer represents a more hydrated region of polymer and surfactant while in the third layer we find mostly very hydrated polymer. In the presence of 0.3 CMC SDS, most of the surfactant is confined within the first two thin layers, while the third layer is best modeled as a thick region of hydrated polymer. Upon addition of more SDS (0.6 CMC) the polymer-only layer shrinks and the total content of polymer in layer 2 is reduced. Consequently the binding of SDS is significantly lower in this layer. Here we note that the SLD for the two blocks $METAC_{90}$ and $(PEO_{45}MEMA)_{100}$ are rather similar, 0.48 and $0.71 \cdot 10^{-6}$ Å^{-2}, respectively. It is therefore not possible to unambiguously determine the location of these segments. However it is likely that the cationic block, $METAC_{90}$ is located closest to the surface.

3.3.2. $(METAC)_m$

Interactions between a pre-adsorbed $(METAC)_m$ layer and SDS were also probed by optical reflectometry, following the experimental procedure used for $(METAC)_m$-*b*-$(PEO_{45}MEMA)_n$. The results obtained for pre-adsorbed layers of $(METAC)_n$ are shown in Fig. 7. Independent of cleaning method, the optical response increases in the presence of 0.3 CMC SDS, where after it levels off. Clearly, SDS adsorbs to reach a plateau value at low concentrations due to electrostatic interactions between positive charges on the polymer chain and the negative charge carried by SDS [45].

We note that the optical response after the final rinsing step is *higher* than that observed prior to SDS addition. This is due to formation of water-insoluble surface attached polyelectrolyte-surfactant complexes that are very difficult to destroy by dilution, as also has been reported in previous studies [46].

3.3.3. $(PEO_{45}MEMA)_n$

The interactions between the uncharged polymer block $(PEO_{45}MEMA)_n$ and SDS were also probed by optical reflectometry following the same procedure as for $(METAC)_m$-*b*-$(PEO_{45}MEMA)_n$, and some results are provided in the Supplementary Information. The effect of SDS is rather limited on both types of silica surfaces, indicating limited incorporation of SDS and limited SDS-induced desorption of the polymer. This may at first seem counterintuitive since PEO homopolymers are known to interact with this surfactant [47]. There are, however, several reasons for this. First, there

Table 6
Structural parameters obtained from fitting a three-layer model to the neutron reflectivity profiles for adsorbed $(METAC)_m$-*b*-$(PEO_{45}MEMA)_n$ layers on silicon before and after sequential addition of SDS.

Layer Parameter[a]	Polymer + SDS (0.3 CMC)	Polymer + SDS (0.6 CMC)
1. $METAC_{90}$ + SDS		
Thickness (Å)	13 ± 2	13 ± 2
Solvent content ($\Phi_{solvent}$, %)	2 ± 1	2 ± 1
Roughness (Å)	4 ± 1	4 ± 1
Adsorbed amount of polymer (mg/m^2)	0.64 ± 0.04	0.67
Adsorbed amount of SDS (mg/m^2)	0.84 ± 0.06	0.81 ± 0.06
2. $METAC_{90}/(PEO_{45}MEMA)_{100}$ + SDS		
Thickness (Å)	25 ± 2	16 ± 2
Solvent content ($\Phi_{solvent}$, %)	89 ± 1	96 ± 1
Roughness (Å)	5 ± 1	4 ± 1
Adsorbed amount of polymer (mg/m^2)	0.18 ± 0.02	0.08 ± 0.01
Adsorbed amount of SDS (mg/m^2)	0.14 ± 0.02	0
3. $(PEO_{45}MEMA)_{100}$		
Thickness (Å)	700 ± 15	100 ± 10
Solvent content ($\Phi_{solvent}$, %)	97 ± 1	97 ± 1
Roughness (Å)	4 ± 1	4 ± 1
Adsorbed amount of polymer (mg/m^2)	2.5 ± 0.1	0.35 ± 0.04

[a] Here we note that the SLD for the two blocks $METAC_{90}$ and $(PEO_{45}MEMA)_{100}$ are rather similar, 0.48 and $0.71 \cdot 10^{-6}$ Å^{-2}, respectively. It is therefore not possible to unambiguously determine the location of these segments. However it is likely that the cationic block, $METAC_{90}$ is located closest to the surface.

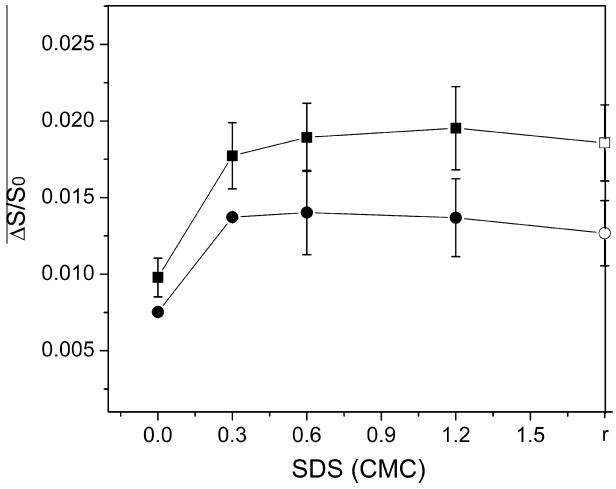

Fig. 7. Optical response $\Delta S/S_0$ (Eq. (2)) as a function of SDS concentration in 10 mM NaCl solutions (pH ~ 6) outside a pre-adsorbed $(METAC)_m$ layer on silica cleaned by Hellmanex (2%) (squares) or, alternatively, Piranha (circles). During formation of the pre-adsorbed layer, the concentration of $(METAC)_m$ was 1 ppm in 10 mM NaCl. The open points denote the values obtained after a final rinsing step with 10 mM NaCl.

is an electrostatic repulsion between SDS and the silica surface, which means that the concentration of SDS next to the surface layer is significantly less than in bulk solution. Further, for brush-like structures the number of adsorbed SDS molecules per ethylene oxide segment decreases rapidly with increasing brush density [48], and we also expect a decreased flexibility of the PEO side chains due to their confinement and partial attachment at the surface that would diminish the interaction with SDS even further.

4. Conclusions

Silica surfaces are often used in fundamental studies as model surfaces due to that they can be prepared to be very smooth, and they are useful for optical, X-ray and neutron reflectivity studies. However, the nature of the silica surface in terms of number and type of silanol groups differ depending on preparation method [24,49]. In this work we demonstrate that silica surfaces cleaned with alkaline solutions are more negatively charged than those cleaned with acidic solutions. As a consequence cationic polyelectrolytes adsorb less on acid cleaned silica surfaces than on alkaline cleaned ones. The structure of the adsorbed layers of $(METAC)_m$-*b*-$(PEO_{45}MEMA)_n$ on silica was characterized by neutron reflectometry. The adsorbed layers were found to have an average thickness of about 700 Å, and the water content of the layer is very high and amounts to 97%. Consistent with theoretical predictions [50], this layer is more extended than those achieved by random copolymers having the same type of segments as $(METAC)_m$-*b*-$(PEO_{45}MEMA)_n$ [7]. The high thickness and water content of the layer is suggested to a consequence of the presence of a high density of strongly hydrated poly(ethylene oxide) side chains, which extend away from the surface forming a branched brush layer structure that has been shown to provide low friction forces up to high pressures in aqueous solutions [12].

The interaction between this pre-adsorbed $(METAC)_m$-*b*-$(PEO_{45}MEMA)_n$ polymer layer and SDS were investigated by neutron reflectometry and by optical reflectometry. From neutron reflectometry, in the presence of low concentration SDS, most of the adsorbed SDS is located close to the silica surface, i.e. in close proximity to the cationic block, while the outer layer is a thick region of hydrated polymer. In the presence of high concentrations of SDS, the content of polymer and SDS is reduced since the outer polymer layer shrinks. The result from optical reflectometry shows that SDS is incorporated in the layer at low SDS concentrations, and more so on alkaline cleaned silica compared to on acid cleaned silica. The higher up-take of SDS also results in more desorption of water-soluble polyelectrolyte-surfactant complexes from this surface at higher SDS concentrations. Thus, we observe that the way the silica surface is cleaned not only affects the adsorbed amount of the oppositely charged diblock copolymer, but also how the layer is affected by addition of anionic surfactant.

Interactions between a pre-adsorbed $(METAC)_m$ layer and SDS studied by optical reflectometry demonstrates that SDS adsorbs to reach a plateau value at low concentrations due to electrostatic interactions between the polymer chain and SDS. The polyelectrolyte-surfactant complexes formed in this case are water-insoluble and therefore limited desorption of SDS occurs during rinsing. This is consistent with previous observations of long-lived polyelectrolyte-surfactant aggregates on mica surfaces after removal of surfactant from bulk solution [46]. Adsorbed layers of the uncharged block, $(PEO_{45}MEMA)_n$, displayed a very limited incorporation of SDS and therefore also limited SDS-induced desorption of the polymer were found. This contrasts to the extensive binding of SDS to linear PEO [51], and is explained by electrostatic repulsion between SDS and the negatively charged silica surface as well as the limited flexibility of the PEO side chains that are adsorbed to the surface.

Acknowledgments

XL acknowledges a stipend from the Chinese Scholarship Council (CSC), PC acknowledges financial support from VR. The project was carried out within the framework of the SSF program "Microstructure, Corrosion and Friction Control". RM gratefully acknowledges financial support from Research Council of Lithuania under the project MIP-51/2012. AD enjoys a VINNMER fellowship from VINNOVA. TN and APD acknowledge support from nmc@LU and VR. The collaboration was facilitated by EU through the NanoS3 project (Grant No. 290251) of the FP7-PEOPLE-2011-ITN call. We also acknowledge the award of beam time on the INTER instrument at the ISIS neutron spallation source (RB1210223).

Appendix A. Supplementary data

Supplementary data associated with this article can be found, in the online version, at http://dx.doi.org/10.1016/j.jcis.2014.11.002.

References

[1] P. Hansson, B. Lindman, Curr. Opin. Colloid Interface Sci. 1 (1996) 604.
[2] S. dos Santos, D. Lundberg, L. Piculell, Soft Matter 7 (2011) 5540.
[3] D.J.F. Taylor, R.K. Thomas, J.D. Hines, K. Humphreys, J. Penfold, Langmuir 18 (2002) 9783.
[4] P.L. Dubin, S.S. The, D.W. McQuigg, C.H. Chew, L.M. Gan, Langmuir 5 (1989) 89.
[5] A.B. Kayitmazer, E. Seyrek, P.L. Dubin, B.A. Staggemeier, J. Phys. Chem. B 107 (2003) 8158.
[6] A. Naderi, R. Makuška, P.M. Claesson, J. Colloid Interface Sci. 323 (2008) 191.
[7] M. Moglianetti, R.A. Campbell, T. Nylander, I. Varga, B. Mohanty, P.M. Claesson, R. Makuska, S. Titmuss, Soft Matter 5 (2009) 3646.
[8] S. Pispas, J. Phys. Chem. B 111 (2007) 8351.
[9] K. Holmberg, B. Jonsson, B. Kronberg, B. Lindman, Surfactants and Polymers in Aqueous Solution, second ed., JohnWiley and Sons, New York, 2002.
[10] X. Liu, A. Dedinaite, M. Rutland, E. Thormann, C. Visnevskij, R. Makuska, P.M. Claesson, Langmuir 28 (2012) 15537.
[11] M. Müller, S. Lee, H.A. Spikes, N.D. Spencer, Tribol. Lett. 15 (2003) 395.
[12] X. Liu, E. Thormann, A. Dedinaite, M. Rutland, C. Visnevskij, R. Makuska, P.M. Claesson, Soft Matter 9 (2013) 5361.
[13] S. Chen, C. Guo, G.-H. Hu, H.-Z. Liu, X.-F. Liang, J. Wang, J.-H. Ma, L. Zheng, Colloid Polym. Sci. 285 (2007) 1543.
[14] A.V. Kabanov, T.K. Bronich, V.A. Kabanov, K. Yu, A. Eisenberg, J. Am. Chem. Soc. 120 (1998) 9941.
[15] L.A. Bastardo, J. Iruthayaraj, M. Lundin, A. Dedinaite, A. Vareikis, R. Makuška, A. van der Wal, I. Furó, V.M. Garamus, P.M. Claesson, J. Colloid Interface Sci. 312 (2007) 21.
[16] A. Naderi, G. Olanya, R. Makuška, P.M. Claesson, J. Colloid Interface Sci. 323 (2008) 223.
[17] P.G. DeGennes, J. Phys. (Paris) 37 (1976) 1445.
[18] R.R. Netz, D. Andelman, Phys. Rep. 380 (2003) 1.
[19] J.-M.Y. Carrillo, A.V. Dobrynin, Langmuir 26 (2010) 18374.
[20] S. Alexander, J. Phys. (Paris) 38 (1977) 983.
[21] M.T.L. Casford, P.B. Davies, D.J. Neivandt, Langmuir 19 (2003) 7386.
[22] E.P.K. Currie, G.J. Fleer, M.A. Cohen, Eur. Phys. J. E 1 (2000) 27.
[23] A. Naderi, J. Iruthayaraj, A. Vareikis, Langmuir 23 (2007) 12222.
[24] G. Olanya, J. Iruthayaraj, E. Poptoshev, R. Makuska, A. Vareikis, P.M. Claesson, Langmuir 24 (2008) 5341.
[25] C. Krasselt, J. Schuster, C. von Borczyskowski, PCCP 13 (2011) 17084.
[26] H.J. Jacobasch, K. Grundke, P. Uhlmann, F. Simon, E. Der, Compos. Interfaces 3 (1995) 293.
[27] K. Fa, V.K. Paruchuri, S.C. Brown, B.M. Moudgil, J.D. Miller, PCCP 7 (2005) 678.
[28] O. Krivosheeva, A. Dėdinaitė, M.B. Linder, R.D. Tilton, P.M. Claesson, Langmuir 29 (2013) 2683.
[29] J.C. Dijt, M.A.C. Stuart, G.J. Fleer, Adv. Colloid Interface Sci. 50 (1994) 79.
[30] T. Dabroś, T.G.M. Van de Ven, Colloid Polym. Sci. 261 (1983) 694.
[31] A. Dėdinaitė, L. Bastardo, Langmuir 18 (2002) 9383.
[32] A. Nelson, J. Appl. Crystallogr. 39 (2006) 273.
[33] J. Ihringer, J. Appl. Crystallogr. 28 (1995) 618.
[34] W.C. Hamilton, Acta Cryst. 18 (1965) 502.
[35] S. Vass, T. Torok, G. Jakli, E. Berecz, J. Phys. Chem. 93 (1989) 6553.
[36] C. Sommer, J.S. Pedersen, P.C. Stein, J. Phys. Chem. B 108 (2004) 6242.
[37] M. Kobayashi, Y. Terayama, M. Hino, K. Ishihara, A. Takahara, JPCS 184 (2009) 012010.
[38] R.K. ILER, The Chemistry of Silica: Solubility, Polymerization, Colloid and Surface Properties and Biochemistry of Silica, John Wiley & Sens, Inc., 1979.
[39] T.K. Wang, R. Audebert, J. Colloid Interface Sci. 121 (1988) 32.
[40] M. Lundin, L. Macakova, A. Dedinaite, P. Claesson, Langmuir 24 (2008) 3814.
[41] K.D. Berglund, T.M. Przybycien, R.D. Tilton, Langmuir 19 (2003) 2705.
[42] E.S. Pagac, D.C. Prieve, R.D. Tilton, Langmuir 14 (1998) 2333.
[43] B. Wittgren, M. Stefansson, B. Porsch, J. Chromatogr. A 1082 (2005) 166.
[44] G. Gunnarsson, B. Joensson, H. Wennerstroem, J. Phys. Chem. 84 (1980) 3114.
[45] K. Pojják, Langmuir 25 (2009) 13336.
[46] A. Dedinaite, P.M. Claesson, M. Bergström, Langmuir 16 (2000) 5257.
[47] B. Cabane, R. Duplessix, J. Phys. France 43 (1982) 1529.
[48] W.M. de Vos, P.M. Biesheuvel, A. de Keizer, J.M. Kleijn, M.A. Cohen, Langmuir 25 (2009) 9252.
[49] G.H. Bolt, J. Phys. Chem. 61 (1957) 1166.
[50] P. Linse, P.M. Claesson, Macromolecules 42 (2009) 6310.
[51] R. Mészáros, I. Varga, T. Gilányi, J. Phys. Chem. B 109 (2005) 13538.